PAGEOPH, Vol. 125, Nos. 2/3 (1987)

0033-4553/87/030341-27$1.50+0.20/0

Substitute Conductors for Electromagnetic Response Estimates

ULRICH SCHMUCKER[1]

Abstract—Various concepts exist to define substitute conductors for empirical response estimates at singular frequencies: Chapman's shell-core model, the Cagniard-Tikhonov apparent resistivity, the Niblett-Bostick and Molochnov transformation, the $\rho^* - z^*$ transformation. They are all interrelated and assign comparable resistivities to the substitute conductor at a given frequency. Applications to synthetic response data of plane and spherical conductors show under which conditions these substitutions come closest to the model and which influence of source dimensions and Earth's sphericity can be expected. $\rho^* - z^*$ transformed global response data for *S* and *Dst* variations demonstrate how substitute conductors may serve as useful guides in inverse procedures.

Key words: Electromagnetic induction, magnetotelluric and geomagnetic sounding, electric conductivity of crust and mantle.

1. Introduction

Substitute conductors essential purpose is to reproduce the electromagnetic response of the conducting Earth to external source fields at one singular frequency. This response can be (i) the Q-ratio of internal to external fields, (ii) the scalar Z-impedance between orthogonal telluric and magnetic horizontal fields, (iii) BANKS' W-ratio of vertical to horizontal magnetic fields which measures the depth of penetration C against lateral source dimensions. All these responses are interrelated and are to be understood as transfer functions between complex FOURIER amplitudes of surface field components.

If amplitude and phase of the response are to be interpreted simultaneously, the substitute conductor must have two adjustable parameters; one of them usually the resistivity of a uniform half-space or sphere. If the phase is ignored, this will be the only parameter to be determined. In either case, different substitutions may have to be adopted for different frequencies. They translate empirical response estimates for a sequence of frequencies with their error limits into sets of model parameters, which as a function of frequency, characterize the true resistivity within the respective depth range of penetration.

After reviewing the basic properties of response functions in Section 2, various concepts to define substitute conductors are presented in Section 3. In Section 4

[1] Institut für Geophysik, Herzberger Landstr. 180, 3400 Göttingen, Federal Republic of Germany.

limitations are considered for conclusions drawn from them, while Section 5 suggests their use as guidelines for inverse procedures.

2. Response Functions

They refer by definition to time and space harmonic electromagnetic fields. For flat Earth models, occupying the lower half-space $z \geq O$ of Cartesian (x, y, z) coordinates, the FOURIER amplitudes of the field components are assumed to have in horizontal planes the time-space factor $\exp\{i(\omega t + k_x x + k_y y)\}$. This introduces a horizontal wavenumber vector $\mathbf{k} = (k_x, k_y)$ to describe the sourcefield geometry with $|\mathbf{k}|^{-1}$ as scale length of source dimensions. For spherical Earth models of radius R, the spherical harmonic $P_n^m(\cos\theta)\exp(im\lambda)$ will express the dependence of the FOURIER amplitudes on colatitude θ and longitude λ on surfaces $r = \text{const.}$ in spherical (r, θ, λ) coordinates. Source dimensions are now given by R/n or, more properly, by $R/\sqrt{n(n+1)}$.

In either case, a laterally uniform Earth is assumed of magnetic permeability $\mu = 1$ throughout. This implies that all responses are directional invariant, i.e., they depend only on the absolute value $|k|$ for a flat Earth and on the degree n of the spherical function for a spherical Earth. Finally, it is assumed that the induction is by tangential electric sources with no vertical or radial electric fields appearing anywhere. Consequently the theory of induction in plane conductors with $\sigma = \sigma(z)$ or in spherical conductors with $\sigma = \sigma(r)$ establishes the following linear relations (see, SCHMUCKER, 1970; WEIDELT, 1972; or ROKITYANSKI, 1982).

Let E and B denote electric telluric and magnetic FOURIER amplitudes in the above sense on surfaces $z = O$ or $r = R$ and let affices (i) and (e) denote their parts from internal and external sources, respectively, with respect to these surfaces. The linear relations which reflect the response of the conducting matter below a flat surface and thus define the response functions $Q = Q(\omega,|k|)$ etc. are

$$\begin{aligned} B_{x,y}^{(i)} &= QB_{x,y}^{(e)}, & B_z^{(i)} &= -QB_z^{(e)} \\ E_x &= +ZB_y, & E_y &= -ZB_x \\ B_z &= iWB_x|k|/k_x, & B_z &= iWB_y|k|/k_y \end{aligned} \tag{1}$$

or

$$B_z = C\{ik_xB_x + ik_yB_y\}$$

with $W = |k|C$.

The corresponding relations for the field on a spherical surface, defining the responses $Q_n(\omega)$ etc. are

$$B^{(i)}_{\theta,\lambda} = Q_n B^{(e)}_{\theta,\lambda}, \qquad B^{(i)}_r = -\frac{n+1}{n} Q_n B^{(e)}_r$$

$$E_\theta = -Z_n B_\lambda, \qquad E_\lambda = +Z_n B_\theta \tag{2}$$

$$B_r = W_n \frac{P^m_n}{dP^m_n/d\theta} B_\theta, \qquad B_r = W_n \frac{\sin\theta}{\mathrm{im}} B_\lambda \; (m \neq 0)$$

or

$$B_r = -\left\{ dB_\theta/d\theta + \cot\theta\, B_\theta + \frac{\mathrm{im}}{\sin\theta} B_\lambda \right\} C_n/R$$

with $W_n = (n+1)nC_n/R$. In deriving the last relation, note that $B_r \sim P^m_n$ and that

$$d^2P^m_n/d\theta^2 + \cot\theta\, dP^m_n/d\theta + \{(n+1)n - m^2/\sin^2\theta\} P^m_n = O.$$

Because electric and magnetic fields are connected also by rot $E = -i\omega B$ and because both fields are continuous at the surface, response functions are interrelated (cf., SCHMUCKER, 1970; BANKS, 1972):

$$Z_{(n)} = i\omega C_{(n)}, \qquad Q = \frac{1 - |k|C}{1 + |k|C} = \frac{1 - W}{1 + W}$$

$$Q_n = \frac{n}{n+1} \frac{1 - (n+1)C_n/R}{1 + nC_n/R} = \frac{n - W_n}{n + 1 + W_n}. \tag{3}$$

Hence, only one of them has to be considered to find substitute conductors. In the following this will be the C-response because of its direct bearing on the penetration depth.

As an example, and for later reference, the C-response of a uniform half-space and sphere is considered, given in *SI* units by

$$C(\omega,|k|) = (i\omega\mu_0\sigma + k^2)^{-1/2} = (2i/p^2 + k^2)^{-1/2}$$

$$C_n(\omega) = Rj_n(i\alpha)/\{i\alpha j_{n-1}(i\alpha) - nj_n(i\alpha)\} \tag{4}$$

with $p = \sqrt{2\rho/\omega\mu_0}$ as 'skindepth' and $\alpha = (1+i)R/p$; j_n denotes modified spherical BESSEL functions of the first kind and order n.

From these expressions the generally valid asymptotic properties of the C-response are readily inferred. Observe that ij_{n-1} is approximately equal to j_n for large arguments $|\alpha|$ and that j_n becomes $(i\alpha)^n/\{1\cdot3\cdot\ldots(2n+1)\}$ for small arguments $|\alpha|$. Allow now, at a sufficiently high frequency, the skindepth to be small against source dimensions as introduced above. Then with $|k|p \ll 1$ and $np/R \ll 1$ the response of plane and spherical conductors approaches the same limiting value

$$C_o(\omega) = \frac{1}{2} p(\omega)\,(1 - i) \tag{5}$$

which is independent of source dimensions. It may be regarded as 'zero-wavenumber' response, but definitely not in the sense that $|k|$ or its spherical equivalent n/R are assumed to be zero, i.e., there will be finite W and Q responses for $C \to C_0$ because—for plane conductors—$dC/dk \to O$ for $|k| \to O$. If to the contrary, $|k| \cdot p$ and $n\ p/R$ are large against unity, a frequency and conductivity independent C-response of 'no induction' is approached: $|k|^{-1}$ for Cartesian coordinates and $R/(n+1)$ for spherical coordinates.

Generalized to any laterally uniform Earth model, the zero-wavenumber approximations

$$C(\omega,|k|), C_n(\omega) \to C_o(\omega) \qquad Z(\omega,|k|), Z_n(\omega) \to Z_o(\omega)$$

$$Q_o(\omega,|k|) \to 1 - 2|k|C_o(\omega) \tag{6}$$

$$Q_n(\omega) \to \frac{n}{n+1}\{1 - (2n+1)C_o(\omega)/R\}$$

apply, when $|C_0| \cdot |k|$ and $n \cdot |C_0|/R_E$ are small against unity; $C_0(\omega)$ denotes now the respective zero-wavenumber response of the model. If these expressions are large against unity, the limiting values for 'no induction' from above apply.

In addition, the C-response of simplified 2-layer models will be needed. Let h be the thickness of a top layer or outer shell above a uniform half-space or sphere of radius $q \cdot R$, $q = 1 - h/R$ with $h \ll R$. Let $p_l = \sqrt{2\rho_l/\omega\mu_o}$ be the skindepth values for the top layer ($l = 1$) and for the uniform substratum ($l = 2$) of resistivity ρ_l. The general formula of the C-response for plane 2-layer models is

$$C(\omega,|k|) = \frac{1}{K_1} \frac{K_1 + K_2 \tanh(K_1 h)}{K_2 + K_1 \tanh(K_1 h)}$$

with

$$K_l^2 = 2i/p_l^2 + k^2 \text{ (e.g., SCHMUCKER, 1970; eq. (5.44)).}$$

Suppose now that the top layer is by comparison a poor conductor, i.e., $p_1 \gg p_2$, and that, at the considered frequency, p_1 is also large against h, but small enough to give $|k|p_1 \ll 1$ and of course also $|k|p_2 \ll 1$. Then with the zero-wavenumber approximations $K_l = (1+i)/p_l$, and with $\tanh(K_1 h) \approx K_1 h$ the C-response from above reduces to

$$C_o(\omega) = h + \frac{p_2(\omega)}{2}(1 - i). \tag{7}$$

The C-response of spherical 2-layer models becomes identical, when $np_l/R \ll 1$ and $h \ll p_1$. Note that in these 'h-type models' the phase of the impedance, $\varphi(\omega) = \arg\{i\omega C_o\}$, lies between 45 and 90 degrees.

Assume for a complementary model that the top layer (or shell) is a thin conductor of conductance $\tau = h/\rho_1$, again with $h/p_1 \ll 1$, but $p_1 \ll p_2$, i.e., the top layer

is by comparison a good conductor. Setting as before kp_l and np_l/R small against unity, the C-response from above has the approximation

$$C_o(\omega) = \frac{p_2(\omega)/(1+i)}{1 + i\omega\mu_o\tau p_2(\omega)/(1+i)} \tag{8}$$

which again is also valid for spherical shell-core models. Note that for this 'τ-type model' the phase of the impedance $\varphi(\omega)$ lies between zero and 45 degrees.

If the uniform substratum is either an extremely good conductor with $p_2 \ll h$ or an extremely poor conductor with $\omega\mu_o\tau p_2 \gg 1$, the C-response for h and τ-models is only determined by their respective parameter h or τ:

$$C_o(\omega) = h, \qquad C_o(\omega) = (i\omega\mu_o\tau)^{-1}. \tag{9}$$

3. *Substitute Conductor Concepts*

Substitute conductors refer exclusively to the zero-wavenumber responses $Q_o(\omega)$, $Z_o(\omega)$ and $C_o(\omega)$ of eq. (6). Their concepts are now listed in chronological order:

3.1 *CHAPMAN'S Uniform-Core Model*

It was introduced to interpret the Q_n responses of a spherically symmetric Earth to solar and lunar daily variations (CHAPMAN and BARTELS, 1942; Section 22.2). The substitute model is an h-type model, consisting of a nonconducting shell of thickness h above a uniform 'core' of radius $q \cdot R$ and resistivity ρ_c. For each time-harmonic of S and L variations Chapman defines a parameter $\beta = qR/p_c(\omega) = qR\sqrt{\omega\mu_o/2\rho_c}$ and observes that the phase of the Q_n-response depends for large values of β almost exclusively on this parameter.

This observation is readily verified from eq. (6) by substituting C_n from eq. (7). The condition $\beta \gg 1$ implies that the zero-wave-number can be used provided that q is near unity:

$$Q_n(\omega) = \frac{n}{n+1}\left\{1 - (2n+1)\frac{h + p_c/2}{R} + (2n+1)\frac{p_c}{2R}i\right\}.$$

Hence for $np_c/R \ll 1$ and $2nh/R \ll 1$, the phase of Q_n is

$$\psi_n(\omega) \approx (2n+1)p_c/2R \tag{10}$$

which is Chapman's eq. (74) for $\beta \gg 1$ and $\mu = 1$. It defines the resistivity ρ_c of the 'core' in terms of phase ψ_n. Similarly, the modulus for sufficiently small phases determines in

$$|Q_n| \approx \frac{n}{n+1}\{1 - (2n+1)(h + p_c/2)/R\}, \tag{11}$$

the thickness of the shell.

An example: Chapman finds for the second time harmonic of S $|Q_n(\omega)| = 1/2.2$ and $\psi_n(\omega) = 18.8$ degrees, $\omega = 4\pi$ *cpd*. The spherical harmonic used for the *m-th* S-harmonic is in Chapman's analysis of degree $n = m + 1$. Thus, with $n = 3$ the following model parameters evolve: $h = 60$ km, $p_c = 597$ km or $\rho_c = 32.6$ Ωm—not far from modern estimates. Chapman quotes on the basis of all S and L harmonics $h = 250$ km and $\rho_c = 27.8$ Ωm.

3.2 The Uniform Substitute Conductor of CAGNIARD-TIKHONOV

This substitution is for magnetotelluric impedance estimates Z, assuming that it is sufficiently close to its zero-wavenumber value Z_o (CAGNIARD, 1953). Since no source geometry enters then into the determination, estimates will be available for a wide range in frequency and the phase information may be thought to be contained in the frequency dependence of $|Z|$. Therefore in this substitution the phase is ignored and, with $|Z| = \omega|C| = \omega p/\sqrt{2}$ from eq. (5), the true Earth is replaced for frequency ω by a uniform conductor of 'apparent resistivity'

$$\rho_a(\omega) = \frac{\mu_o}{\omega}|Z|^2 = \omega\mu_o|C|^2 \tag{12}$$

at zero depth.

BERDICHEVSKY and DMITRIEV give the following interpretation of $\rho_a(\omega)$: Obtain the squared telluric surface amplitude $|E|^2$, $E = E_x$ or E_y, by integration over its derivatives, with respect to depth z:

$$|E(O)|^2 = -\int_o^\infty \{\partial|E|^2/\partial z\}\, dz = -\int_o^\infty \{2|E|\partial|E|/\partial z\}\, dz.$$

Substitute E by $\pm\mu_o^{-1}\rho\partial B/\partial z$ (from rot $\mathbf{B} = \mu_o E/\rho$ for a laterally uniform field) and $\partial E/\partial z$ by $\pm i\omega B$ (from rot b.f. $= -i\omega B$) with B standing for B_x or B_y. This gives with $|E|^2/|B|^2$ for $|Z|^2$ at $z = 0$

$$\rho_a = -\int_o^\infty \rho\{\partial|B(z)/B(O)|^2/\partial z\}\, dz$$

and, with corresponding substitutions in $\partial|B|^2/\partial z$, for the apparent conductivity

$$\sigma_a = \rho_a^{-1} = -\int_o^\infty \sigma\{\partial|E(z)/E(O)|^2/\partial z\}\, dz.$$

The apparent resistivity or conductivity thus sample the true Earth resistivity or conductivity according to the attenuation which the squared magnetic or electric field undergo as functions of depth.

3.3 The NIBLETT-BOSTICK Transformation

It assigns the substitute resistivity ρ_{NB} to the depth $|C|$, taking frequency derivatives of $|C|$ into account. No specific model is used and this transformation does not attempt to find a substitute conductor which reproduces the observed response. Instead NIBLETT (1960) defines for the depth range down to $z = |C(\omega)|$ the conductance

$$\tau_{NB}(\omega) = \int_{o}^{|C(\omega)|} \{\rho_{NB}(z)\}^{-1}\, dz$$

in terms of the substitute resistivity to be found. Regarding this depth range as 'thin sheet' and assuming that the remaining half-space $z \geq |C|$ is an extremely poor conductor, eq. (9) applies and connects τ_{NB} with $|C|$:

$$\tau_{NB}(\omega) = \{\omega\mu_o|C(\omega)|\}^{-1}.$$

Differentiating both relations with respect to ω leads in

$$\{\rho_{NB}(|C|)\}^{-1} d|C|/d\omega = -\frac{d|C|/d\omega + |C|/\omega}{\omega\mu_o|C|^2}$$

to an expression which defines ρ_{NB} at depth $|C(\omega)|$. Rewriting it for $\rho_a = \omega\mu_o|C|^2$ and $d\rho_a/d\omega$ gives

$$\rho_{NB}\{|C(\omega)|\} = \rho_a(\omega)\frac{1 + m(\omega)}{1 - m(\omega)} \tag{13}$$

with $m = -\omega/\rho_a \cdot d\rho_a/d\omega$. WEIDELT's 3rd inequality (WEIDELT, 1972; eq. (2.32)) ensures that for consistent response estimates $|m|$ does not exceed unity.

The same inequality implies a monotonic increase of $|C|$ with decreasing frequency, i.e., the transformation should give a depth profile $\rho_{NB}(|C|)$ which with decreasing frequency continues monotonically downwards.

Because $d|C|/d\omega$ is not an observable quantity and error estimates are difficult to assign to it, WEIDELT's formula

$$\varphi \approx \frac{\pi}{4}(1 - m)$$

(WEIDELT, 1972; eq. (2.28)) presents the possibility to approximate $m(\omega)$ by the phase $\varphi(\omega)$ and its well defined error. With $\Phi = \varphi - \pi/4$ as phase difference against the phase of uniform conductors, the approximated transformation becomes

$$\rho_{NB} = \rho_a \frac{1 - \frac{4}{\pi}\Phi}{1 + \frac{4}{\pi}\Phi} \tag{13a}$$

or, for small phase differences,

$$\rho_{NB} \approx \rho_a(1 - \frac{8}{\pi}\Phi). \tag{13b}$$

3.4 *The MOLOCHNOV Transformation*

It defines with similar arguments a substitute resistivity ρ_M for depth $|C|$, but uses a different modeling concept, yielding

$$\rho_M = \rho_a(1 + m)^2 = \rho_{NB}(1 - m^2) \tag{14}$$

(MOLOCHNOV, 1968). Obviously, both transformations lead to similar results for $m \ll 1$. Because ρ_M will always be smaller than ρ_{NB} (for $m \neq 0$), this substitution reproduces the true resistivity better than ρ_{NB}, when the resistivity decreases downward ($m < O$), but less well where the resistivity increases with depth ($m > O$).

3.5 *The* $\rho^* - z^*$ Transformation

It is based on plane 2-layer models with two adjustable parameters: an h-model according to eq. (7) for response estimates with a phase $\varphi = \arg\{\dot{Z}\}$ above 45 degrees, a τ-model according to eq. (8) when this phase is below 45 degrees. In the original concept (SCHMUCKER, 1970; KUCKES, 1973) h-models were used in both cases. The supplementary τ-model was added later (SCHMUCKER, 1971; Sec. 3.2).

Let ρ^* denote in either model the resistivity of the underlying uniform half-space with skindepth $p^* = \sqrt{2\rho^*/\omega\mu_o}$. Then for $\varphi \geq \pi/4$, thickness h^* of the resistive top layer and skindepth p^* of the uniform half-space follow readily from eq. (7) as

$$\begin{aligned} h^*(\omega) &= \mathrm{Re}\{C(\omega)\} + \mathrm{Im}\{C(\omega)\} \\ p^*(\omega) &= -2\,\mathrm{Im}\{C(\omega)\} \end{aligned} \tag{15}$$

which gives the half-space resistivity as

$$\rho^*(\omega) = 2\omega\mu_o(\mathrm{Im}\{C(\omega)\})^2 = 2\rho_a(\omega)\cos^2\varphi(\omega) \tag{16}$$

with $\arg\{C\} = \varphi - \pi/2$ and ρ_a from eq. (12).

If $\varphi \leq \pi/4$, the model parameter of the τ-model are found with similar expressions from the admittance $A = Z^{-1}$. Replacing C in eq. (8) by $A = (i\omega C)^{-1}$ leads with τ^* as top layer conductance and

$$A = \mu_o\tau^* + \frac{1 - i}{\omega p^*} \tag{17}$$

to

$$\mu_o \tau^*(\omega) = \mathrm{Re}\{\mathrm{A}(\omega)\} + \mathrm{Im}\{\mathrm{A}(\omega)\}$$
$$p^*(\omega) = -(\omega\ \mathrm{Im}\{\mathrm{A}(\omega)\})^{-1} \tag{18}$$

and, with $\arg\{\mathrm{A}\} = -\varphi$, to the complementary definition

$$\rho^*(\omega) = \frac{1}{2}\frac{\mu_o}{\omega}/\mathrm{Im}\{A(\omega)\}^2 = \frac{1}{2}\rho_a(\omega)/\sin^2\varphi(\omega). \tag{19}$$

Thus, by the use of phase information, a new apparent half-space resistivity $\rho^*(\omega)$ is found, which is freed from the influence of surface layers, providing at the same time in $h^*(\omega)$ or $\tau^*(\omega)$ estimates of thickness or conductance of these layers.

By joining ρ^*-values from a sequence of frequencies, a depth profile $\rho^* - z^*$ can be constructed by assigning $\rho^*(\omega)$ as a substitute resistivity to the frequency depending depth $z^*(\omega) = \mathrm{Re}\{C(\omega)\}$ of a perfect substitute conductor, eq. (9). This conductor would produce the in-phase part of the internal magnetic surface field and z^* is therefore an indicator of the depth from which the in-phase induction currents flow at the respective frequency.

WEIDELT's 2nd inequality (WEIDELT, 1972; eq. (2.31)] ensures that z^* increases monotonically with decreasing frequency. Furthermore, if $\hat{\imath}_u(z)$ denotes the density of the in-phase currents at a given frequency, the integral $\int_o^{\infty} \hat{\imath}_u(z - z)\, dz$ is zero for any laterally uniform half-space (WEIDELT 1972; Sec. 2g). This establishes the depth z^* as 'center depth of the in-phase currents' in the sense of a center of mass, even though there will be weak currents with a phase of 180 degrees and negative densities $\hat{\imath}_u$ at some greater depth. The choice of z^* as depth estimate for ρ^* comes from models with an exponentially decreasing resistivity as discussed in Sec. 4.5.

3.6 Comparison

This section concludes with a comparison of the various substitutions. Chapman's procedure is identical with the $\rho^* - z^*$ transformation, if the phase φ is close to 90 degrees and $\mathrm{Im}\{C\}$ about equal to $|C|$ $(\frac{\pi}{2} - \varphi)$.

There exists also a simple relationship between the NIBLETT-BOSTICK and the $\rho^* - z^*$ transformation, when the phase φ is not too far from 45 degrees. Expressing ρ^* from eqs. (15) and (19) in terms of the phase difference $\Phi = \varphi - \pi/4$ leads to

$$\rho^* = \rho_a \cdot \begin{cases} (1 - \sin 2\Phi)\ , & \Phi \geq O \\ (1 + \sin 2\Phi)^{-1}, & \Phi \leq O \end{cases} \tag{20}$$

Hence, for small values of Φ, ρ^* approaches $\rho_a(1 - 2\Phi)$ whereas from eq. (13b) $\rho_{NB} \rightarrow \rho_a(1—8/\pi \cdot \Phi)$, implying a 25% larger deviation of ρ_{NB} from ρ_a. But since ρ_{NB} is assigned to a larger depth $|C|$ than ρ^*, both transformations will not be too different, if the resistivity changes monotonically with depth.

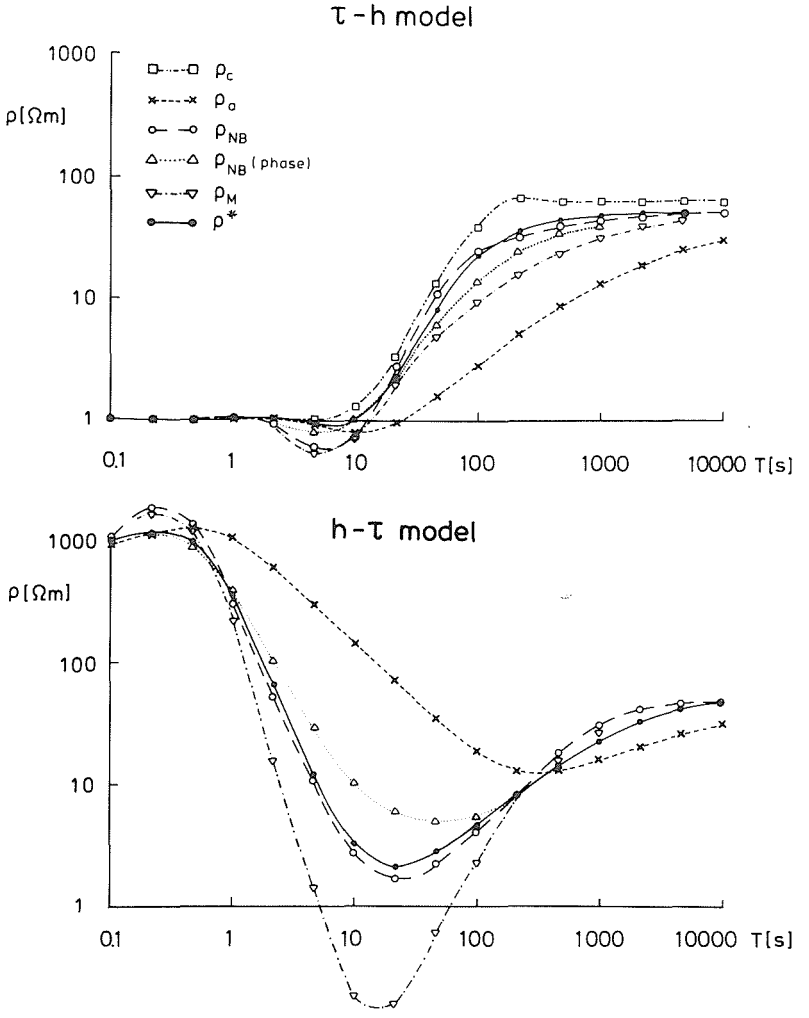

Figure 1

Comparison of various concepts to define substitute resistivities for the zero-wavenumber response. The chosen model response is for the two 3-layer models of Figure 4 over five decades in period T.—ρ_c: CHAPMANs 'core' resistivity; ρ_a: CAGNIARD-TIKHONOV apparent resistivity; ρ_{NB}: NIBLETT-BOSTICK resistivity, also as phase-approximation eq. (13a); ρ_M: MOLOCHNOV resistivity; ρ^*: h, τ-model resistivity.

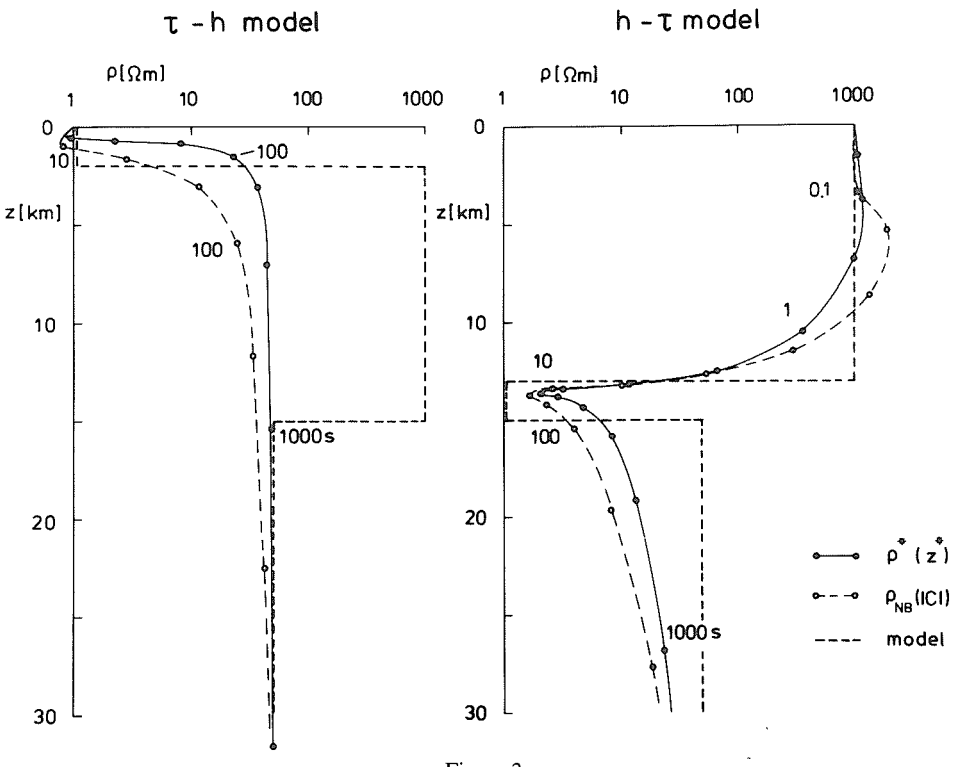

Figure 2

NIBLETT-BOSTICK transformation and $\rho^* - z^*$ transformation of the zero-wavenumber response of the same models as in Figure 1. Curve parameter is the period T. The transformations both reproduce the right-hand model, but not the intermediate high resistivity layer in the left-hand model. Note in either case the shielding which conductors exert upon underlying poor conductors, evidenced by large deviations of ρ_{NB} and ρ^* from the true resistivity.

To illustrate these relationships, substitutions are carried out with response data of two models (Figure 1 and 2). They are combined h- τ-models, in which a highly resistive top layer is underlain by a thin conductive sheet above a uniform half-space or *vice versa* with the thin sheet on top. The combined responses follow from eqs. (7) and (8) as

$$C_o(\omega) = h + \frac{p/(1+i)}{1 + i\omega\mu_o\tau p/(1+i)} \tag{21a}$$

for the $h - \tau$ model and as

$$C_o(\omega) = \frac{h + p/(1+i)}{1 + i\omega\mu_o\tau\{h + p/(1+i)\}} \tag{21b}$$

for the $\tau - h$ model. The intercomparison uses, however, not these approximations, but the exact formula for 3-layer models with finite values assigned to all model parameters. Substitutions requiring $d|C|/d\omega$ have been carried out with analytically derived frequency derivatives. For comparison, phases Φ also have been used in their place. To include Chapman's 'core' resistivity ρ_c, the approximation for $\mathrm{Im}\{C\}$ from above was employed.

Figure 1 shows the substitute resistivities from all definitions as functions of period $T = 2\pi/\omega$. They all reveal the essentials of the respective model, even though those with phase information more distinctively and within a narrower range in period. However note that the poorly conducting intermediate layer in the $\tau - h$ model is hardly resolved. In Figure 2 the same responses are converted into $\rho_{NB}(|C|)$ and $\rho^*(z^*)$ plots. Both transformations lead to comparable depth profiles in which the intermediate good conductor of the $h - \tau$ model appears at about the correct depth, while the intermediate poor conductor of the $\tau - h$ model is not visible. This inherent and irrevocable limitation in the resolving power of electromagnetic response data will be considered in greater detail in the following section.

4. Application to Response Functions of Models

The transformation of response estimates into substitute conductors provides insight into the class of models which is to be studied for final interpretation. Limitations are twofold: from the limited resolving power of response functions as such and from finite source dimension. They are considered now on the basis of models of variable complexity, resembling real Earth conditions. The substitution to be used is the $\rho^* - z^*$ transformation from Sec. 3.5.

4.1 2-Layer Models

These are plane Earth models with great resistivity contrasts in the sense that, at sufficiently low frequency, the top layer acts either as nonconductor ('h-model') or as thin-sheet conductor ('τ-model'). The chosen top layer resistivities of 1000 and 1 Ωm, respectively, are representative values for crystalline rocks and well-conducting sediments. With a thickness of 15 and 2 km the top layers may resemble the upper crust or a sedimentary basin above a moderately conducting substructure, here given a resistivity of 50 Ωm.

Figure 3 shows the $\rho^* - z^*$ transformed model responses over five decades in period $T = 2\pi/\omega$. Responses over three decades, here from 1 to 1000s, are sufficient to derive all model parameters directly from a visual display of the $h^*(T)$, $\tau^*(T)$ and $\rho^*(T)$ curves. The response at longer periods alone would determine only thickness or conductance of the top layer and the half-space resistivity. Nearly correct values are then obtainable from the response at just one singular frequency.

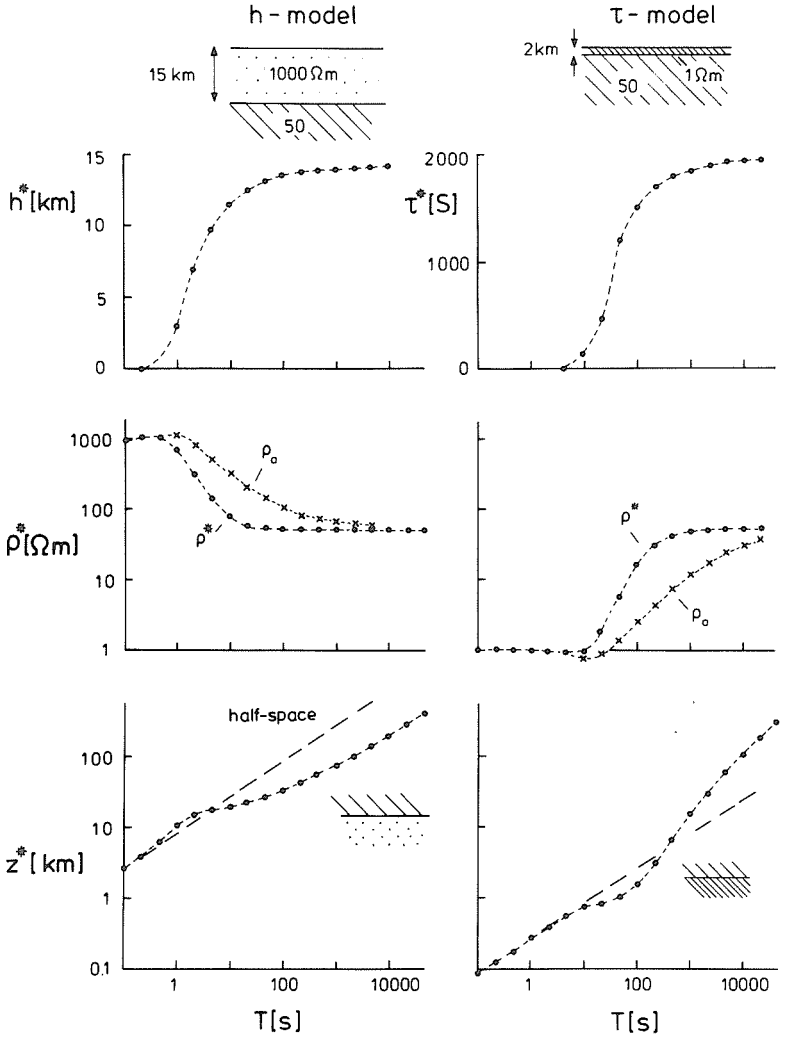

Figure 3

$\rho^* - z^*$ transformation of the response of plane 2-layer models over five decades in period T. From top to bottom: the model, thickness or conductance estimates for the top layer, estimated resistivity ρ^* for the half-space (for comparison also the apparent resistivity ρ_a), depth of the perfect substitute conductor.

The display of the depth $z^*(T)$ of the perfect substitute conductor illustrates how the center depth of the in-phase induced currents moves downward with increasing period. Where this curve levels off in relation to the indicated uniform half-space slope $z^* = p/2 \sim \sqrt{T}$, the bottom or top of a good conductor is reached, slowing down the descent of the currents to greater depth. Where the $z^*(T)$ curve is steeper, the currents pass more quickly through a depth range of high resistivity.

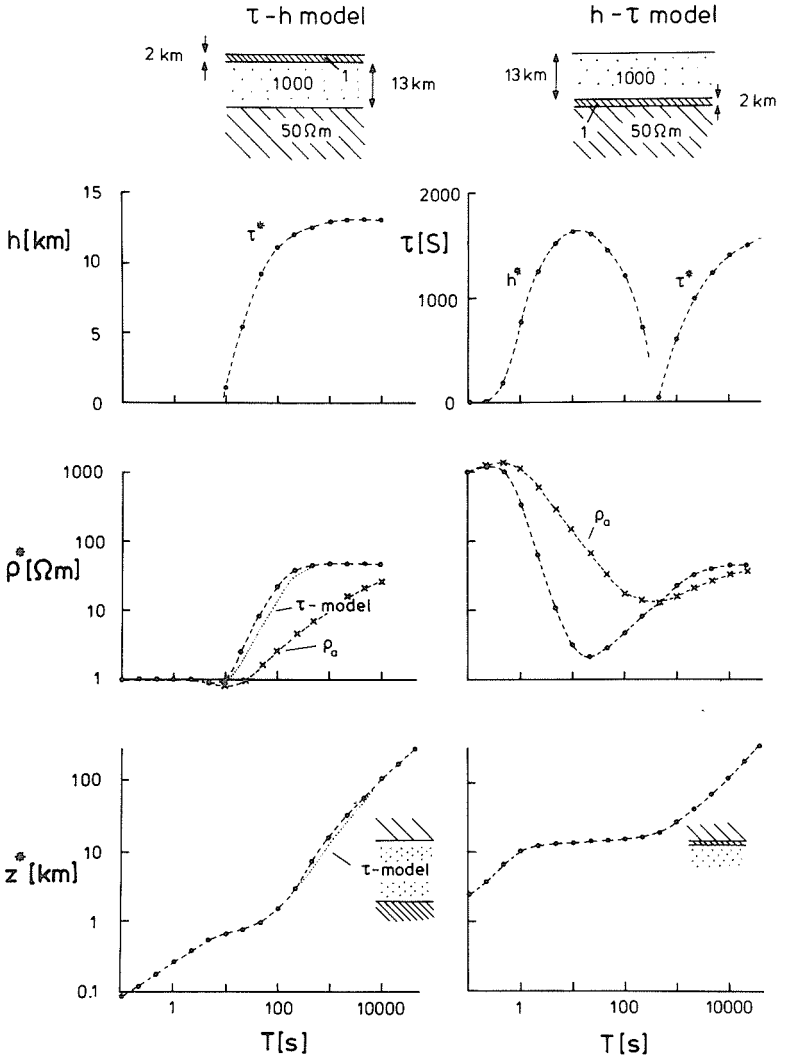

Figure 4

$\rho^* - z^*$ transformation of the response of plane 3-layer models. See Figure 3 for further explanations.—While both top layers are well resolved, in the model to the right, the second layer of high resistivity in the model to the left is not recognizable in the transformed response curves.

4.2 3-Layer Models

They are combined h- and τ-models, i.e., the resistivity contrasts are again sufficiently large so that the two top layers become at long periods effective nonconductors or thin-sheet conductors. The $\tau - h$ model to the left in Figure 4 represents the typical case that well-conducting sediments overlie highly resistive basement rocks;

the $h - \tau$ model to the right the case of a thin mid-crustal conductor below such basement rocks in the absence of sediments. The following conclusions are readily verified from eqs. (21).

In the $\tau - h$ model the resolving power of the response is now limited due to the shielding which the good conductor at the top exerts on the poor conductor below. In fact, this second layer is totally invisible. At long periods τ^* merges into the correct conductance of the first layer. But at shorter periods, when the phase is barely above 45 degrees, there is no indication from h^* values for the mere existence of a second layer, nor does this evidence come from ρ^* at any period. Where the center depth of induced currents passes through the depth range of the poor conductor, the slope of the $z^*(T)$ curve is indeed slightly increased, but again the difference against the τ-model without such a conductor is minute.

A reversed sequence of the top layers restores in the $h - \tau$ model the resolving power of the response. There are now sections with h^* at short periods ($\varphi > \pi/4$) and with τ^* at long period ($\varphi < \pi/4$) which give unambiguous evidence for the existence of two top layers, providing almost correct values for their thickness and conductance. The same can be inferred from ρ^* and z^*, which level off quite visibly at the correct depth of the thin conductor. In summary, conductance and thickness of the top layers, as well as the half-space resistivity, are well determined model parameters. Responses at very short periods would establish also a finite top layer resistivity, while thickness and resistivity of the second layer remain uncertain except for the fact that it acts like a thin-sheet and has a known conductance.

4.3 Multi-layer Models

If such models are constructed from a sequence of h and τ-conductors, PARKER's model (1980) evolve which can reproduce any given set of response data. But it becomes increasingly difficult to identify individual layer parameters just from a visual inspection of h^*/τ^*, ρ^* or z^*-curves. It may be even difficult to estimate only the right number of layers, as it was demonstrated for the case of $\tau - h$ models, and only inverse procedures can yield at least an approximate answer (cf., Sec. 5).

4.4 Continuous Models

They provide an alternative way for a direct interpretation of response data, if not more than two or three adjustable parameters are involved. Firstly, models with a monotonic increase or decrease of resistivity with depth will be studied, i.e., exponential or power law models. They have been instrumental in the original formulation of the $\rho^* - z^*$ transformation (SCHMUCKER, 1970; KUCKES 1973). LAHIRI and PRICE (1939) used such analytic models to interpret the global Q-response of S-and *Dst* variations (cf. Figure 7).

Consider then a model with an exponentially decreasing resistivity: $\rho(z) = \rho_0$

$\exp(-2\lambda z), \lambda > O$. Let $E(z)$ denote the complex FOURIER amplitude of the tangential electric field (E_x or $-E_y$) at depth z. Then, for a zero-wavenumber approximation, the C-response has to be found from the solution of

$$d^2E/dz^2 = \alpha^2\lambda^2 e^{2\lambda z}E$$

with

$$\alpha = \sqrt{i\omega\mu_o/\rho_o}/\lambda = (1 + i)/(p\lambda)$$

and $p = \sqrt{2\rho_o/\omega\mu_o}$ as skindepth at zero depth. The substitution $u = \exp(\lambda z)$ converts this equation into

$$u^2d^2E/du^2 + udE/du - \alpha^2u^2E = O,$$

which has as a solution modified Bessel functions of order zero. Those of the second kind have the right behaviour for $u, z \to \infty$:

$$E(u) = A \cdot K_o(\alpha u) \text{ with } E(\infty) = O.$$

The tangential magnetic field B (for B_y or B_x) follows from $\partial E/\partial z = -\alpha\lambda uAK_1(\alpha u) = -i\omega B$ and gives at $z = O$ ($u = 1$) the desired response:

$$C_o(\omega) = i\omega\frac{E(1)}{B(1)} = \frac{1}{\alpha\lambda}K_o(\alpha)/K_1(\alpha). \tag{22}$$

In order to see how well the $\rho^* - z^*$ transformed response resembles the model, two limiting cases are considered. At sufficiently high frequency and shallow depth of penetrations $p\lambda$ will be small and $|\alpha|$ large against unity. The appropriate approximations for Bessel functions yield

$$K_o(\alpha)/K_1(\alpha) = 1 - 1/2\alpha + 3/8\alpha^2 + O\{\alpha^{-3}\}$$

and thereby

$$C_o = \frac{p}{2}\left\{1 - i + \frac{1}{2}\lambda pi - \frac{3}{16}(\lambda p)^2(1 + i)\right\}. \tag{23}$$

Since the phase $\varphi = \pi/2 - \arg\{C_o\}$ is above 45 degrees, eqs. (15) are to be used, yielding the substitute resistivity

$$\rho^*(z^*) = \rho_o\{1 - \lambda p + \frac{5}{8}(\lambda p)^2\}$$

for depth $z^* = p/2 \cdot \{1 - 3/16\ (\lambda p)^2\}$ to second order in (λp). The model resistivity at this depth is, again to second order,

$$\rho(z^*) = \rho_o{}^{-2\lambda z^*} \approx \rho_o\left\{1 - \lambda p + \frac{1}{2}(\lambda p)^2\right\},$$

i.e., the $\rho^* - z^*$ transformation reproduces the shallow part of the model quite correctly with a small difference in the second order term.

At low frequencies and great depth of penetration $p\lambda$ will be large against unity and $|\alpha|$ small. The appropriate approximations are now $K_o = -ln(\alpha)$ and $K_1 = \alpha^{-1}$, which when inserted into eq. (22) give

$$C_o = -ln(\alpha)/\lambda = ln\left(\frac{p\lambda}{1+i}\right)/\lambda \tag{24}$$

and therefrom the substitute resistivity eq. (16)

$$\rho^*(z^*) = \omega\mu_o\, \pi^2/8 \cdot \lambda^{-2}$$

for depth

$$z^* = ln\{p\lambda\sqrt{2}\}/\lambda.$$

A comparison with the model value

$$\rho(z^*) = 2\rho_o/(\lambda p)^2 = \omega\mu_o/\lambda^2$$

reveals again a remarkable fit, except for a constant factor of $\pi^2/8 = 1.23$, independent of depth and model parameter λ or p. Since in the intermediate frequency range also no larger deviations occur, as demonstrated in Figure 9, the substitution provides a close approximation to the true resistivity at all depth.

To first order in λp, the model parameter can be derived—as in the case of 2 layer models—directly from the response at one singular frequency:

$$p = 2\mathrm{Re}\{C_o\},\ \lambda p = 4(\mathrm{Re}\{C_o\} + \mathrm{Im}\{C_o\}) \tag{23a}$$

at high frequencies from eq. (23) and

$$\lambda^{-1} = -4/\pi \cdot \mathrm{Im}\{C_o\},\ \lambda p = \sqrt{2}\exp(\lambda\, \mathrm{Re}\{C_o\}) \tag{24a}$$

at low frequencies from eq. (24).

KUCKES (1973) came with power law models $\rho(z) \sim z^{-m}$, $m > O$, to similar conclusions and, as Figure 6 shows, the Lahiri and Price power law model for a spherical Earth is also well represented by $\rho^* - z^*$ transformed S and Dst responses, calculated for this model. If an overlying effective nonconductor or thin-sheet conductor shall be included, simply add its thickness to the C-response of eq. (22) or its conductance, multiplied with μ_o, to the admittance $A = 1/i\omega C$.

Models with an exponentially increasing resistivity $\rho(z) = \rho_o \exp(2\lambda z)$, $\lambda > O$, are treated in similar ways. By substitution of $u(z) = \exp(-\lambda z)$ the solution is now in terms of modified Bessel functions of the first kind: $E(u) = AI_o(\alpha u)$ with α from eq. (22) and $E(0) = A$, yielding from $i\omega B(u) = \alpha\lambda I_1$ as C-response

$$C_o(\omega) = \frac{1}{\alpha\lambda} I_o(\alpha)/I_1(\alpha). \tag{25}$$

Note that the electric field has a finite value at $z = \infty$, reflecting the problematic zero-wavenumber approximation, when σ is or approaches zero at infinite depth.

For simplicity, it may be assumed that source dimensions are infinite.

Using again the approximations for large arguments $|\alpha|$, the high-frequency response becomes

$$C_o(\omega) = \frac{p}{2}\{1 - i - \frac{1}{2}\lambda p i - \frac{3}{16}(\lambda p)^2(1 + i)\}, \tag{26}$$

i.e., the phase is below 45 degrees and the substitute resistivity ρ^* has to be derived from the admittance according to eq. (19). This gives

$$\rho^*(z^*) = \rho_o\left\{1 + \lambda p + \frac{5}{8}(\lambda p)^2\right\}$$

for depth $z^* = p/2\ \{1 - 3/16\ (\lambda p)^2\}$, which again agrees well to second order in λp with the correct resistivity

$$\rho(z^*) \approx \rho_o\left\{1 + \lambda p + \frac{1}{2}(\lambda p)^2\right\}$$

at that depth.

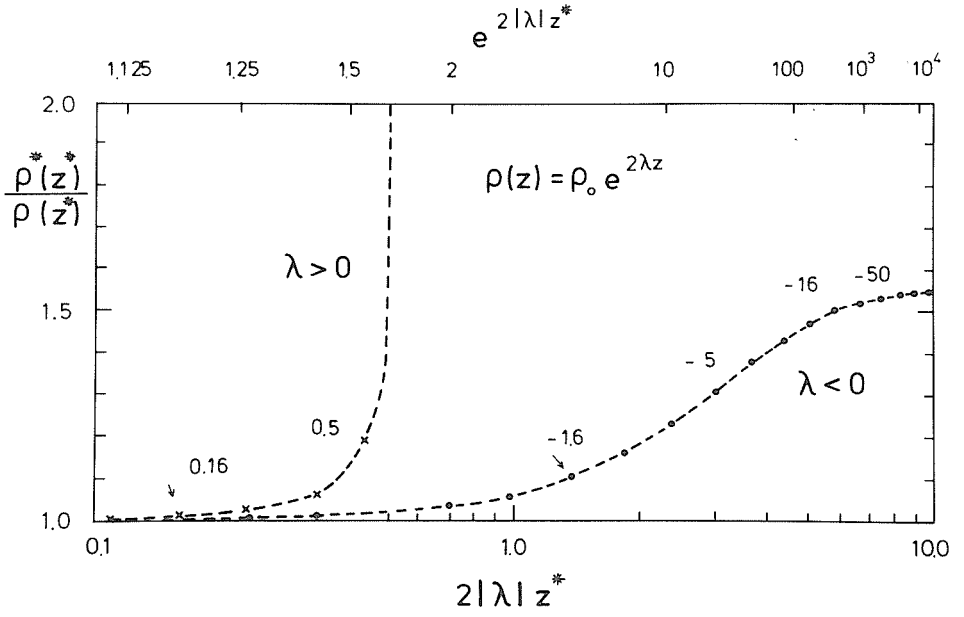

Figure 5

$\rho^*(z^*)$-resistivity in relation to the true resistivity $\rho(z^*)$ as function of the exponent in exponential models. On top the resistivity at depth z^* in relation to the surface resistivity ρ_o. Curve parameter is λp with p as skindepth for ρ_o, i.e., the period and depth of penetration increase along the curves from the left to the right. Since the response, multiplied with λ, depends only on λp (cf., eqs. (22) and (25)), the shape of the curves is the same for all exponential models with a shifted curve parameter λ.—While ρ^* never deviates more than by a factor of 1.5 from the true resistivity at any depth, when the resistivity is exponentially decreasing (λ negative), such agreement exists only at short periods with $\lambda p \leq 0.5$, when the resistivity is exponentially increasing (λ positive).

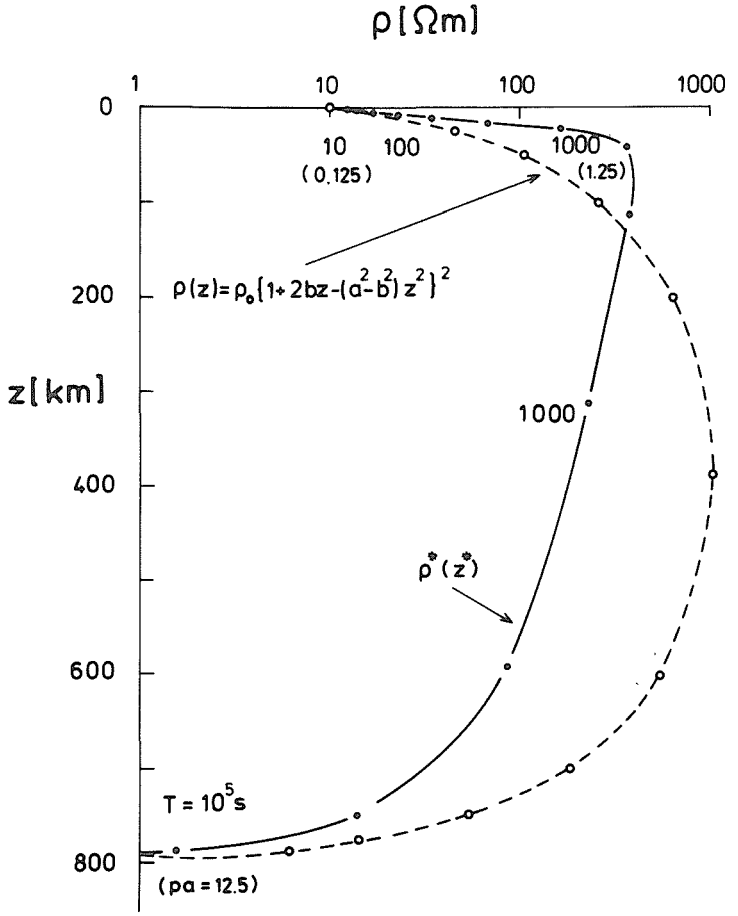

Figure 6

$\rho^* - z^*$ transformation of the response for a continuous model with maximal resistivity at 388 km, zero resistivity at 800 km and $\rho_o = 10$ Ωm at zero depth ($a^{-1} = 40$ km, $b = 0.95 \cdot a$). The transformed response between 100 000s and 10s reproduces the uppermost and lowermost portion of the model near the ultimate depth of 800 km, when $p \cdot a = \sqrt{2\rho_o/\omega\mu_o} \cdot a$ is either small or large against unity. In the intermediate depth range ρ^* is at first above the model until a cross-over at $pa \sim 2.8$, and then below.

For small arguments the approximations $I_o(\alpha) = 1 + (\alpha/2)^2$ and $I_1(\alpha) = \alpha/2 \cdot \{1 + \frac{1}{2}(\alpha/2)^2\}$ lead to the, not quite realistic low frequency response

$$C_o(\omega) = -ip^2\lambda + 1/4\lambda \tag{27}$$

and from the admittance to the substitute resistivity

$$\rho^*(z^*) = 16\rho_o \cdot (p\lambda)^6$$

at constant depth $z^* = (4\lambda)^{-1}$. This is in total disagreement with the model, similar to KERTZ's (1978) conclusion in a corresponding 2-layer case with a nonconducting substratum. Due to shielding by shallow low resistivities, the increasingly poor conductor at depth is not resolvable. The fields simply do not penetrate deeply enough (Figure 5).

Finally, power series models are considered which have maximum resistivity at some intermediate depth. Appropriate fourth order polynomials of the form

$$\rho(z) = \rho_o \{1 + 2bz - (a^2 - b^2)z^2\}^2 \quad a > b > O, \qquad z \leq (a - b)^{-1},$$

have an analytically derivable response: From WEIDELT (1972, eqs. (2.16)/(2.17))

$$C_o(\omega) = p/\{\sqrt{(pa)^2 + 2i} - pb\} \tag{28}$$

with $p = \sqrt{2\rho_o/\omega\mu_o}$ as zero depth skindepth. The model starts off with a surface value ρ_o, reaches at depth $b/(a^2 - b^2)$ a peak value $\rho_o/\{1 - (b/a)^2\}^2$ and approaches zero resistivity at depth $z = (a - b)^{-1}$. As it is readily verified from the high and low frequency approximations of eq. (28), when $p{\cdot}a$ is either small or large against unity, there is again a good agreement between the substitute conductor $\rho^*(z^*)$ and the model at shallow and great depth near $(a - b)^{-1}$. But, as Figure 6 shows, ρ^* does not reach the peak resistivity at intermediate depth, demonstrating once again the basic limitations of substitute conductors, when shielding by low resistivities near the surface is involved.

4.5 Source Effects

They are of second order in depth of penetration versus source dimensions. For uniform Earth models this is verified by approximating their responses in eq. (4) to second order in (kp) and (np/R), respectively:

$$\begin{aligned} C(\omega,k) &= C_o(\omega){\cdot}\{1 + (kp/2)^2 i\} \\ C_n(\omega) &= C_o(\omega){\cdot}\{1 + n(n+1)(p/2R)^2 i\} \end{aligned} \tag{29}$$

In the case of the spherical conductor second order approximations in α^{-1},

$$j_n(i\alpha) = i^n e^\alpha / 2\alpha \left[1 - \frac{n(n+1)}{2\alpha} + \frac{n(n+1){\cdot}\{n(n+1) - 2\}}{(2\alpha)^2 2} \right],$$

for spherical Bessel functions with large arguments$|\alpha|$ were used.

This result can be generalized to any Earth model, but excluded are plane models which approach or have infinite resistivity at infinite depth. PRICE (1962) based his assessment of source effects mainly on models of this type, where this effect is unavoidable. But since realistic Earth models always conclude with a good conductor at some ultimate depth, source effects will not exceed those from uniform conductors.

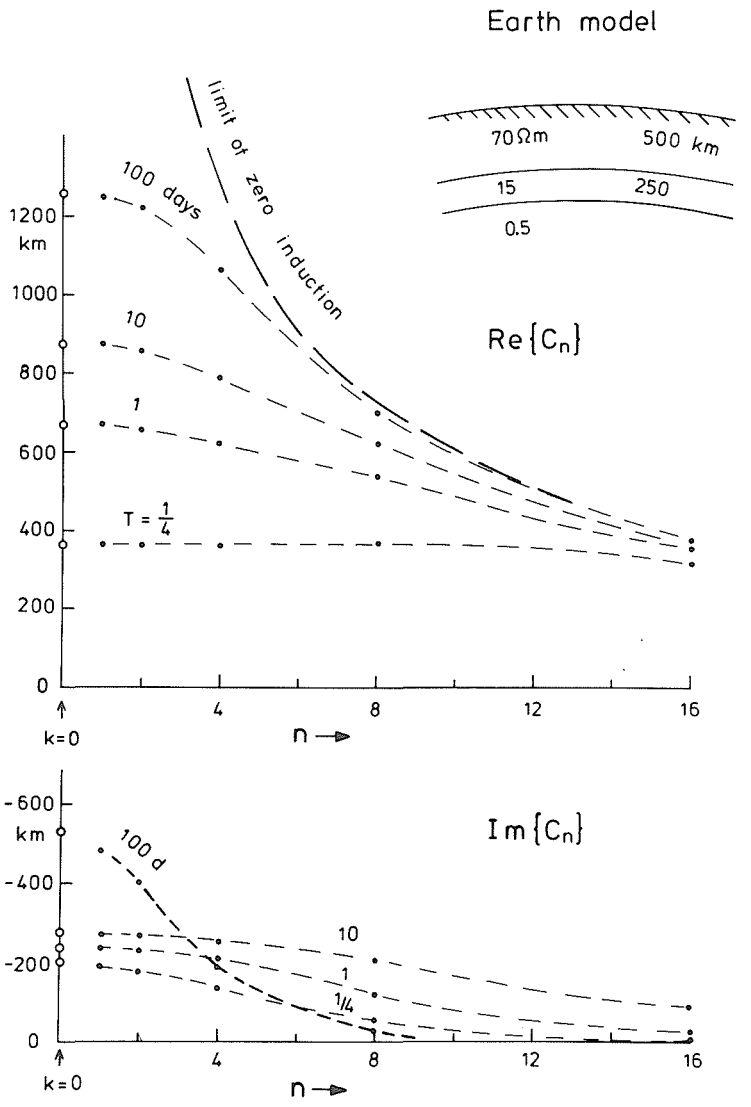

Figure 7

Source effect on the C-response of the 3-layer spherical Earth model A from Figure 11. The real and imaginary parts of the calculated response function $C_n(\omega)$ is shown for increasing degrees of spherical harmonics of the source until the limit of 'no-induction' $C_n = R/(n + 1)$ is reached, $R = 6371$ km. Curve parameter is the period T in days.—The source dependence of the real part of C_n is up to $n = 16$ very small for variations with T smaller than 6 hours, but clearly visible in the imaginary part and thus in the phase of the response. For periods of one and ten days source dimensions affect also the real part, but for n less than about 4 the response is far from its limiting value of 'no-induction', i.e., mainly determined by the internal resistivity distribution. For $T = 100$ days this limit is practically reached, when n exceeds 4.

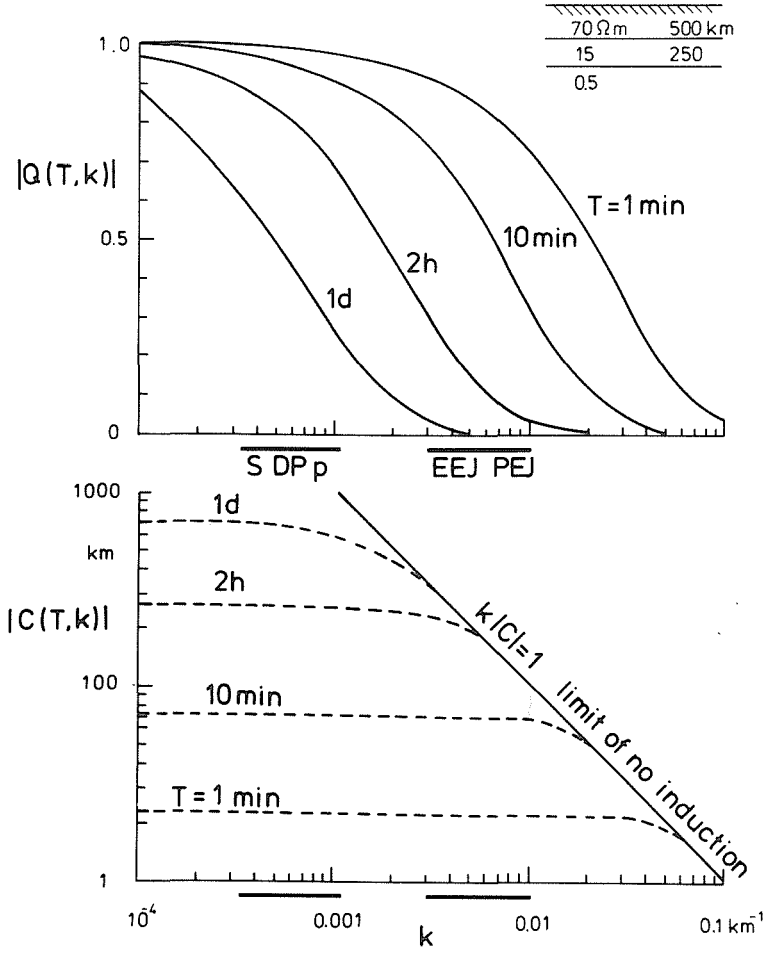

Figure 8

Source effect on the Q and C-response of plane 3-layer Earth model A from Figure 11, shown for the moduli as function of horizontal wavenumber k for fast and slow variations. Bars indicate the spectral range in k for slow and fast variations in mid-latitudes (left) and in jet regions (right). The ultimate wavenumber for ground observations should be 0.01 km^{-1} corresponding to source dimensions of 100 km which is the height of the nearest source region in the ionospheric E-layer.—For the chosen Earth model, source effects on the C-response will be neglible for pulsations everywhere, but note that their internal part is visibly below $Q = 1$ in jet regions, i.e., their depth of penetration will become here comparable to source dimensions without marked effect on C, however. Slow variations in jet regions, on the other hand, are close to the limit of 'no-induction' $Q = O$ and $C = k_j^{-1}$ their use for electromagnetic investigations is therefore critically dependent on the exact knowledge of the spatial source configuration. In mid-latitudes only very slow variations have a slightly source-dependent C-response, but note again the clearly reduced Q-response against unity, which allows response estimates also from magnetic vertical variations.

This is demonstrated in Figure 7 for the C-response of the spherical Earth model from Sec. 5, in Figure 8 for the Q- and C-response of an equivalent plane model. It appears that the zero-wave-number response is a valid approximation throughout except for slow DP and S variations in jet regions. In the period range of diurnal variations jet fields are close to the limit of 'no induction', i.e., they are without any significant internal part, where the chosen Earth model applies.

If source dimensions are known and independent of frequency, WEIDELT's transformation formulas (1972; Sec. 3) can be used to convert response estimates $C(\omega,k)$ or $C_n(\omega)$ into zero-wavenumber responses $C_o(\omega)$. However this is not possible for diurnal variations, for instance, because each time harmonic requires spherical harmonics of different degrees n. But, as Figure 9 shows, source effects and effects

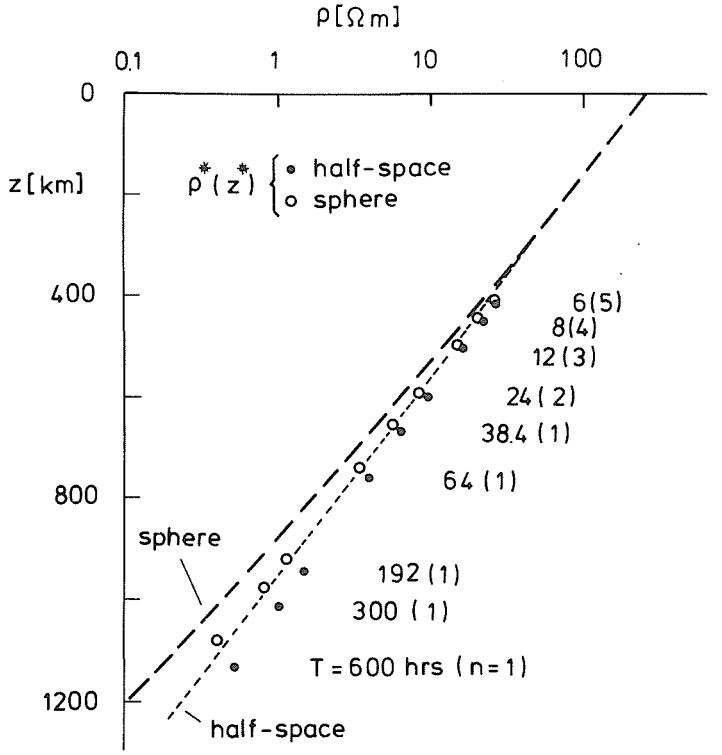

Figure 9

$\rho^* - z^*$ transformation of the model response, when the resistivity decreases in the Earth's mantle exponentially with depth. To demonstrate, how source dimensions and sphericity influence the response, two models are compared: (i) a spherical model $\rho(z) = \rho_o\{1 - z/R\}^m$ and a source field of variable degrees n of spherical harmonics, as indicated; (ii) a plane model $\rho(z) = \exp\{-2\lambda R\}$ and a quasi-uniform source field, $k = 0$. With $\rho_o = 250$ Ωm, $m = 37$, $R = 6371$ km and $2\lambda = m/R$ the models represent model 'd' by LAHIRI and PRICE (1939) to interpret global response estimates for S and Dst variations. See Table 1 for such estimates at the selected periods from 6 to 600 hours.

from the Earth's sphericity are small even for these deeply penetrating variations of rather complicated source field structure.

5. *Application to Response Estimates from Observations*

They refer to discrete frequencies and are from a harmonic analysis of regular variations or from a spectral analysis of irregular variations. In either case, averages of squared, spectral amplitudes are involved which assigns *rms* errors δ to response function estimates from a sequence of frequencies or frequency bands. They apply as relative errors to the modulus or as absolute errors to the phase, i.e., in the case of the C-response either an error $\delta|C|$ is assigned to $|C|$ or an error δ in angular measure to the phase. Since all definitions of substitute and apparent resistivities involve the squared modulus, their relative errors are 2δ, assuming the phase to be correct. Similarly, the relative errors of h^*, τ^* and z^* are δ.

The selected sample data set consists of response estimates for S and *Dst* variations at nine frequencies, ranging in period T from 6 hours for the 4-th Sq-harmonic to 600 hours for the *Dst*-continuum near the spectral peak from the 27-day reoccurrence tendency of magnetic storms. They have been derived from 18 months of observation at 13 European observatories, which are not situated on or near the coast, and have been taken from a recent collection of such data (SCHMUCKER, (1985); Tables 6 and 7, Sec. 4.2.2, column 'SCH').

Table 1 lists the response estimates and their transformation into substitute conductor resistivities. All phases are clearly above 45 degrees and, as Figure 10 shows, a simple h-type model will apply. The $h^*(T)$ curve merges into a constant depth of 750 km which would be the top of the underlying good mantle conductor.

Table 1

Sq *and* Dst *response estimates for continental Europe*

T hrs	C km		δ	ρ_a Ωm	φ degrees	h^* km	ρ^* Ωm
6	365	$-215i$	0.12	66 ± 16	60 ± 7	150 ± 20	34 ± 8
8	405	$-295i$	0.07	69 ± 10	54 ± 4	110 ± 10	48 ± 7
12	565	$-320i$	0.04	77 ± 6	60 ± 3	245 ± 10	37 ± 3
24	750	$-155i$	0.05	54 ± 5	78 ± 4	600 ± 30	4.4 ± 0.4
38.4	690	$-150i$	0.06	28 ± 3	78 ± 5	540 ± 30	2.6 ± 0.3
64	780	$-160i$	0.05	22 ± 2	78 ± 4	620 ± 30	1.8 ± 0.2
192	860	$-120i$	0.05	8.6 ± 0.9	82 ± 4	740 ± 40	0.3 ± 0.03
300	900	$-200i$	0.09	6.2 ± 1.1	77 ± 7	700 ± 60	0.6 ± 0.1
600	1020	$-290i$	0.12	4.1 ± 1.0	74 ± 9	730 ± 90	0.6 ± 0.2

The $\rho^*(T)$ assigns to it a half-space resistivity of 0.6 Ωm, while the overlying top layer appears to have a resistivity in excess of 50 Ωm. In the $z^*(T)$ curve an incon-

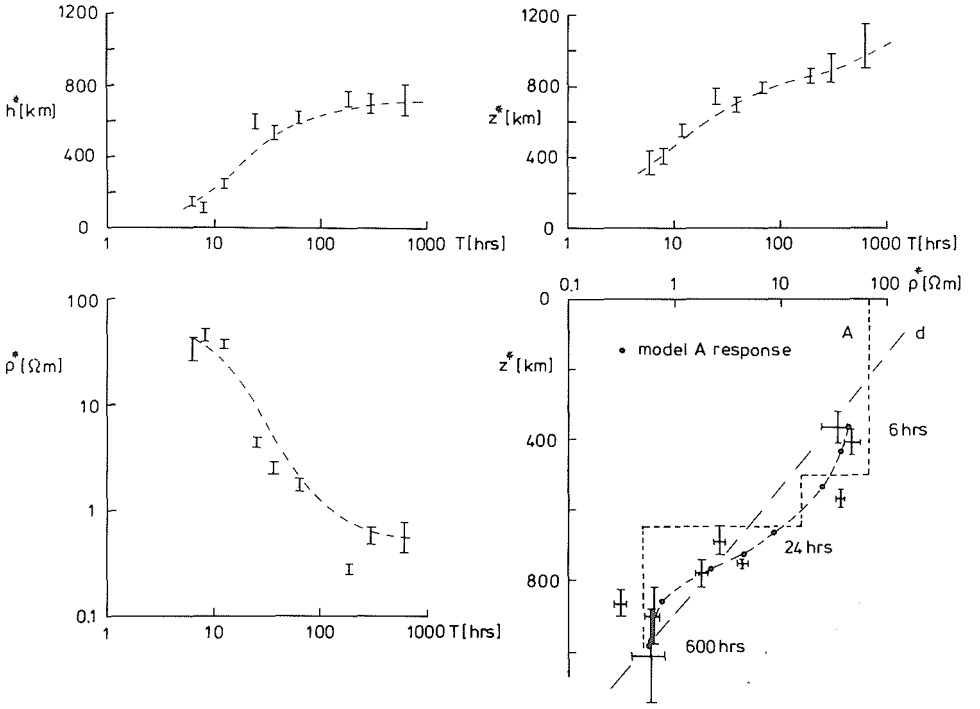

Figure 10

$\rho^* - z^*$ transformation of nine response estimates for S and Dst variations, derived from vertical to horizontal magnetic variations at twelve continental European observatories (Table 1). The estimates range in period from $T = 6$ to 24 hours in S and from 38.4 to 600 hours (= 25 days) in Dst.—The transition depth from high to low mantle resistivity is well established by a nearly constant h^*-values of 700 km at long periods, also by the reduced slope of $z^*(T)$ around that depth. From $\rho^*(T)$ follows at short periods a mean upper mantle resistivity above 50 Ωm and from ρ^* at long periods a mean lower mantle resistivity below 1 Ωm. The $\rho^* - z^*$ plot combines these depth and resistivity estimates into a smoothed image of the mantle resistivity distribution below the European continent.—Empirical estimates are compared with calculated $\rho^* - z^*$ values for the 3-layer model A from Figure 11. For comparison the LAHIRI-PRICE model 'd' (without surface conductor) is shown. But note that its $\rho^* - z^*$ would have followed closely the model line (cf. Figure 9), while the empirical values are in better agreement with the response of the step model A.

sistency is noticeable, when at the transition from Sq to Dst the depth of the perfect substitute conductor decreases slightly with increasing frequency, but the reduced slope between 600 and 800 km depth clearly indicates, where the transition to low mantle resistivities occurs.

The interpretation by layered models allows three or four layers at the most (Figure 11). If a continuous Earth model with an exponential decrease in resistivity $\rho_o \exp(-2\lambda z)$ is adopted, the response at the longest period (600 hrs) gives from eq.

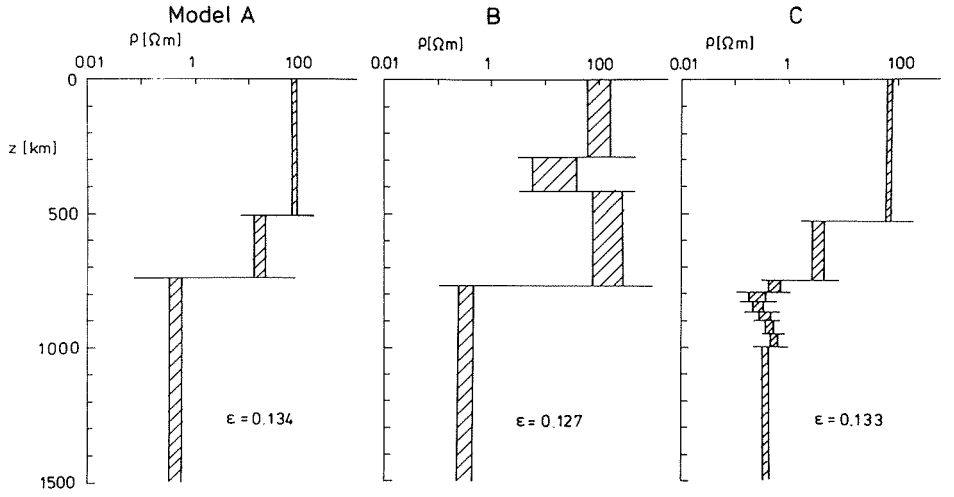

Figure 11

Least squares model interpretation of the response data in Table 1 by layered spheres. For details cf. SCHMUCKER (1985)—Model A: The best fitting 3-layer model with the constraint that layer thickness times square root of layer conductivity is an adjustable constant to minimize the quoted *rms* misfit ε between observed and calculated logarithmic responses, i.e., model A explains the data within 13.4% which is roughly also the *rms* error of the data. Models B and C with additional layers (model C from a generalized inversion) do not improve the fit, but are thought to bring out possible details which seem to be supported by certain characteristics of the data: A reduced resistivity in the uppermost mantle and a thin conducting zone in the transition region between the high and low resistivity region of the mantle, starting at 750 km depth.

(24a) the following parameter: $\lambda = 2.71 \cdot 10^{-3}$ km^{-1}, $p = 8270$ km, $\rho_o = 125$ Ωm. Converting it into a spherical power law model $\rho_o(1 - z/R)^m$, then from the equivalence of both models for $z \ll R$ the exponent $m = 2\lambda R = 34.5$ evolves which is close to $m = 37$ in the LAHIRI and PRICE model 'd'.

Since $\lambda p = 22.4$ is well above unity, the low frequency approximation is justified. For verification by the high frequency approximation $\lambda p \ll 1$, responses at less than one hour period would be needed, which are not available.

Finally, the $\rho^* - z^*$ plot in Figure 10 will be examined again to see, whether the data might yield further resolvable properties beyond an interpretation by two or three uniform layers. There are indeed indications for such properties, the first from the slightly reduced ρ^* value of the 4-th *Sq* harmonic, the second from the *Dst* response at 192 hours or 8 days, which has the smallest imaginary part of all responses. The first indication is for an upward reduction of resistivity, when moving into the depth range of less than 400 km, the second indication is for a thin zone of extremely low resistivity at 800 km depth, where the transition takes places from high to low mantle resistivity.

But it will be noted that both indications are from response estimates at only one frequency, i.e., attempts to use more complicated models, as shown also in Figure 11, will not improve the overall fit between observed and calculated responses to any extent. On the other hand, such models are not only compatible with the data within error limits, but they are also a motive for further investigations.

This concludes the final discussion regarding how substitute conductors, as a direct expression of the collected data, guide the search for models which fully exploit their information content. But regardless of the specific inverse procedure used for the final interpretation, it should not produce models with properties which are not visible already in the data themselves.

References

BANKS, R. J. (1972), *The Overall Conductivity Distribution of the Earth.* J. Geomagn. Geoelectr. *24*, 337–351.

CAGNIARD, L. (1953), *Basic Theory of the Magnetotelluric Method of Geophysical Prospecting.* Geophysics *18*, 605–635.

CHAPMAN, S. and BARTELS, J., *Geomagnetism.* (Oxford Clarendon Press 1940) 1049 pp.

KERTZ, W. (1978), *Das $\rho^*(z^*)$-Verfahren bei mit der Tiefe zunehmendem Widerstand.* Protokoll Kolloq. Erdmagnetische Tiefensondierung, Neustadt/Weinstraße, Nieders. Landesamt f. Bodenforschung Hannover, 77–80.

KUCKES, A. F. (1973), *Relations Between Electrical Conductivity of a Mantle and Fluctuating Magnetic Fields.* Geophys. J. R. Astr. Soc. *32*, 119–131.

LAHIRI, B. N. and PRICE A. T. (1939), *Electromagnetic Induction in Non-uniform Conductors and the Determination of the Conductivity of the Earth from Terrestrial Magnetic Variations.* Phil. Trans. Roy. Soc. London *A 237*, 509–540.

MOLOCHNOV, G. V. (1968), *Magnetotelluric Sounding Interpretation Using the Effective Depth of Penetration of Electromagnetic Fields*, in Russian. Izv. Akad. Nauk SSSR Fiz. Semli *9*, 88–94.

NIBLETT, E. R. and SAYN-WITTGENSTEIN, C. (1960), *Variation of Electrical Conductivity with Depth by the Magnetotelluric Method.* Geophys. *25*, 998–1008.

PARKER, R. L. (1980), *The Inverse Problem of Electromagnetic Induction: Existence and Construction of Solutions Based on Incomplete Data. J. Geophys. Res. 85*, 4421–4428.

PRICE, A. T. (1962), *The Theory of Magnetotelluric Methods when the Source Field is Considered.* J. Geophys. Res. *67*, 1907–1918.

ROKITYANSKY, I. I., *Geoelectromagnetic Investigation of the Earth's Crust and Mantle* (Springer-Verlag, Berlin–Heidelberg–New York 1982) 381 pp.

SCHMUCKER, U. (1970), *Anomalies of Geomagnetic Variations in the Southwestern United States.* Scripps Institution of Oceanography Bulletin *13*, Univ. of California Press, 165 pp.

SCHMUCKER, U. (1971), *Neue Rechenmethoden zur Tiefensondierung.* Protokoll Kolloq. Erdmagnetische Tiefensondierung Rothenberge, Inst. für Geophysik Göttingen, 1–39.

SCHMUCKER, U., *Magnetic and electric fields due to electromagnetic induction by external sources, Electrical Properties of the Earth's Interior*, Landolt-Börnstein (Numerical Data and Functional Relationships in Science and Technology) New Series Group V Vol. 2b (Springer-Verlag 1985).

WEIDELT, P. (1972), *The Inverse Problem of Geomagnetic Induction.* Z. f. Geophysik *38*, 257–289.

(Received 20th January, 1987, accepted 21st January, 1987)